This article has been cited by:

1. Toshitaka Yoshii , Andrea E. Hafeman , Jeffry S. Nyman , Javier M. Esparza , Kenichi Shinomiya , Dan M. Spengler , Gregory R. Mundy , Gloria E. Gutierrez , Scott A. Guelcher . A Sustained Release of Lovastatin from Biodegradable, Elastomeric Polyurethane Scaffolds for Enhanced Bone RegenerationA Sustained Release of Lovastatin from Biodegradable, Elastomeric Polyurethane Scaffolds for Enhanced Bone Regeneration. *Tissue Engineering Part A*, ahead of print. [Abstract] [Full Text] [PDF] [PDF Plus]
2. Toshitaka Yoshii , Shinichi Sotome , Ichiro Torigoe , Hidetsugu Maehara , Yumi Sugata , Tsuyoshi Yamada , Kenichi Shinomiya , Atsushi Okawa . 2010. Isolation of Osteogenic Progenitor Cells from Trabecular Bone for Bone Tissue EngineeringIsolation of Osteogenic Progenitor Cells from Trabecular Bone for Bone Tissue Engineering. *Tissue Engineering Part A* **16**:3, 933-942. [Abstract] [Full Text] [PDF] [PDF Plus]

OPLLによる脊髄障害への電気生理学的アプローチ

川端 茂徳*1) 大川 淳*2) 富澤 將司*3) 四宮 謙一*4)

連続型や混合型の骨化を有する後縦靱帯骨化症（ossification of posterior longitudinal ligament：OPLL）では，MRIなど各種画像診断のみでは障害責任高位を正確に診断することは困難である。術前に脊髄機能を知ることは重要であり，このような場合，電気生理学的な脊髄機能診断が有用である。

また，脊椎靱帯骨化症の症例ではほかの疾患に比して手術中に脊髄障害をきたす危険性が高く，安全に手術をおこなうには脊髄モニタリングが必須である。

Updates of Ossification of Posterior Longitudinal Ligament.

Electrophysiological diagnosis of spinal cord dysfunction in ossification of posterior longitudinal ligament.

Department of Orthopaedic Surgery, Tokyo Medical and Dental University.

Shigenori Kawabata, Atsushi Okawa, Shoji Tomizawa, Kenichi Shinomiya

It is extremely difficult to make a correct diagnosis of the responsible lesion in multilevel continuous and mixed-type ossification of the posterior longitudinal ligament (OPLL) even after magnetic resonance imaging (MRI). Understanding the function of the preoperative spinal cord is crucial for surgical planning and electrophysiological diagnosis of spinal cord function is useful in such cases. Also, intraoperative spinal cord monitoring is required for cervical OPLL surgery because OPLL patients show postoperative neurological deterioration more frequently than any other pathogenesis.

はじめに

後縦靱帯骨化症（ossification of posterior longitudinal ligament：OPLL）は重篤な脊髄障害の原因となることが多く，適切な診断に基づいた治療方法が求められる。脊髄圧迫があるが機能障害をきたしていない症例や，骨化巣が多椎間に

*東京医科歯科大学整形外科 1)（かわばた・しげのり） 2) 准教授（おおかわ・あつし） 3)（とみざわ・しょうじ） 4) 教授（しのみや・けんいち）

及ぶ場合は，各種画像診断や神経学的所見のみでは診断が困難であることも多く，電気生理学的検査が確定診断の助けとなる。

また脊椎靱帯骨化症例では，ほかの疾患に比して手術中に脊髄障害をきたす危険性が高く，安全に手術をおこなうには術中脊髄モニタリングが有用である。

頸椎 OPLL 症例における電気生理学的診断[1)2)]

脊髄の電気生理学的機能診断法としては，体性感覚誘発電位（SEP），末梢神経伝導検査（M波，F波），経頭蓋磁気刺激－筋誘発電位，針筋電図検査などが一般的におこなわれている。これらの検査法で大まかに脊髄機能障害の有無が診断でき，OPLL による脊髄圧迫により脊髄機能障害が起きているかの診断に有用である。

多椎間におよぶ OPLL で詳細に脊髄機能障害高位を診断する必要がある場合は，これらの検査では高位診断は困難であり，脊髄誘発電位測定が必要となる。脊髄誘発電位は体表からでは測定が困難であるため，脊髄近傍のくも膜下腔・硬膜外腔，椎間板内，黄色靱帯内などに電極を設置する必要がある（**図1**）。胸髄刺激後の脊髄刺激脊髄誘発電位（SP-SCEP）では後索・後側索を上行する

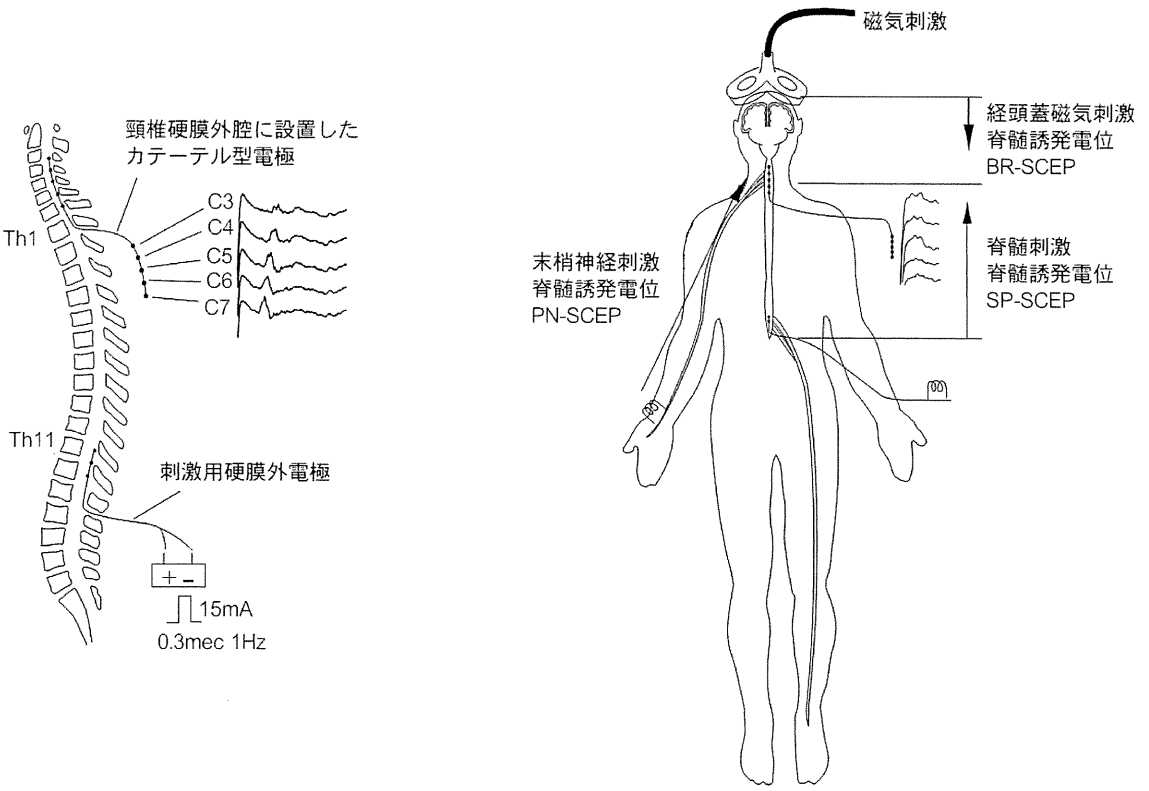

図1　各種脊髄誘発電位の模式図

記録電極は，硬膜外腔・くも膜下腔・黄色靱帯・椎間板内など脊髄近傍に設置する。脊髄・脳・末梢神経を刺激し，脊髄誘発電位を記録する。

（筆者ら作成）

OPLL：ossification of posterior longitudinal ligament（後縦靱帯骨化症），SEP：体性感覚誘発電位

電位，脳を電気または磁気で刺激することで索路を下行する経頭蓋刺激脊髄誘発電位（BR-SCEP）を記録できる。上肢末梢神経幹刺激後の脊髄誘発電位（PN-SCEP）では髄節性電位（神経根枝の電位，シナプス電位，索路の電位の混合電位）を記録することができる。これらの電位の振幅の変化や

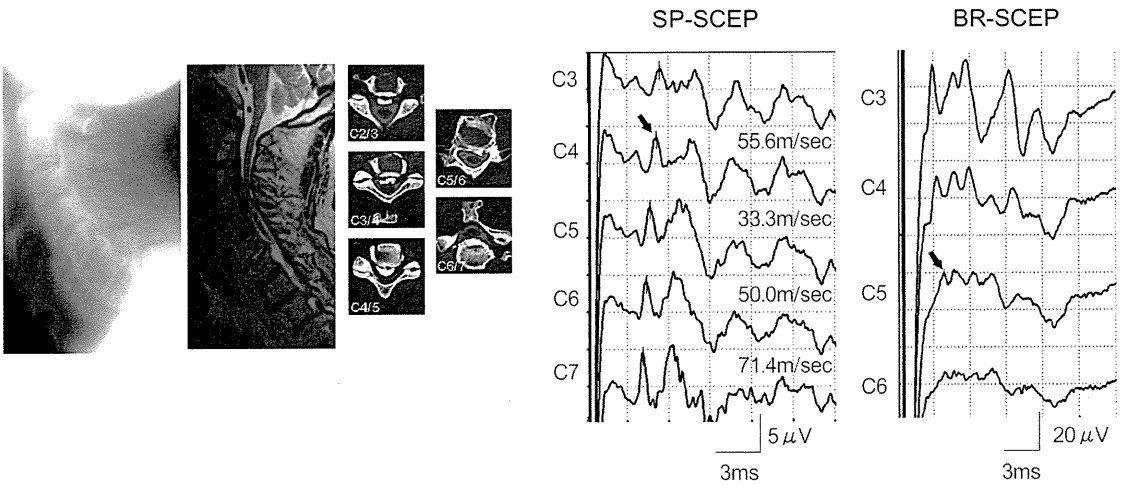

図2　症例1　72歳男性 C2-6，6-7 OPLL

主訴：四肢しびれ，歩行障害，膀胱直腸障害
上行性のSP-SCEP，下行性のBR-SCEPともに最狭窄部のC4/5で電位変化があり，機能障害部位と診断される。
（筆者ら作成）

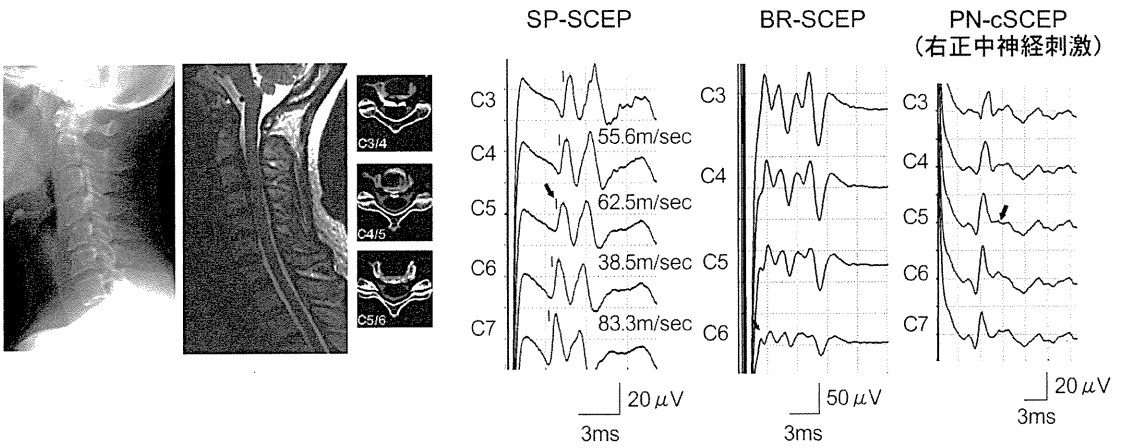

図3　症例2　56歳女性 混合型 OPLL C2-4，5-6

主訴：頸部痛，四肢しびれ
最狭窄部はC3/4であるが，電位測定ではC5/6障害の診断であった。
（筆者ら作成）

BR-SCEP：経頭蓋刺激脊髄誘発電位，PN-SCEP：脊髄誘発電位，SP-SCEP：脊髄刺激脊髄誘発電位

潜時遅延をみることで，多椎間におよぶOPLLにおいても，詳細に脊髄機能障害部位を診断することができる（図2，3）。

OPLLの形態と脊髄障害高位の関係[3)4)]

当院の頸椎OPLL患者について，脊髄誘発電位による脊髄障害高位診断結果と骨化形態の関係について検討した。骨化形態が限局型の症例はすべて骨化に一致した最狭窄高位で障害を認めた。連続型骨化の症例では障害タイプは多様で，骨化の切れ目や骨化の上下端など動的因子が関与する部位で機能障害をきたす例，最狭窄部で機能障害をきたす例，両者が混合し多髄節で障害されている例があった。分節型・混合型でも同様に多様な障害タイプを呈したが，特に多髄節障害は混合型OPLLに多かった（図4）。このように，頸椎OPLLによる脊髄障害の原因は動的因子と静的因子の両因子がともに関与し複雑な症状を呈していることが少なくない。

OPLL症例における術中脊髄モニタリング（図5，6）[5)6)]

広範囲の骨化や骨化占拠率の大きい靱帯骨化症では除圧手術中の神経障害の危険も高い。当院で1997～2003年に頸椎OPLLの手術を行った73例中5例（6.4%）に術後神経症状の悪化を認めている。内訳は脊髄障害3例，C5麻痺が1例，遅発性C5麻痺1例であった。これはそのほかの脊髄症手術例の神経合併症（1.5%）に比べ明らかに多かった。

術中障害の回避には術中脊髄モニタリングが有用である。我々はBR-SCEP，経頭蓋電気刺激筋誘発電位（BR-MSEP），SEPを組み合わせてモニタリングをおこなっている。術中のモニタリング

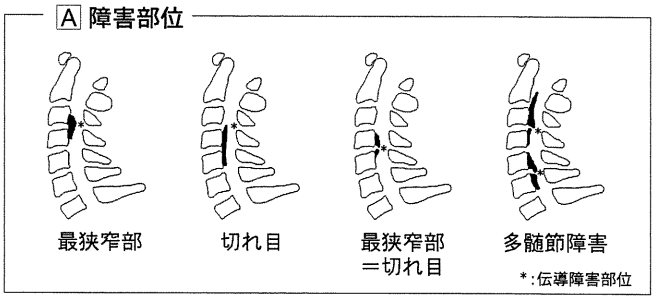

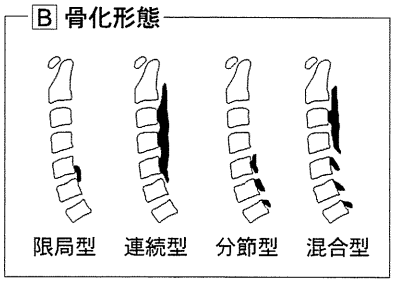

C	最狭窄部	切れ目	最狭窄部＝切れ目	多髄節障害	計
限局型	4	—	—	—	4
連続型	1	2	—	1	4
分節型	3	1	2	—	6
混合型	—	5	3	6	14
計	8	8	5	7	28

図4　骨化形態と障害高位の関係

伝導障害部位を骨化との関係から上記Aの4つのタイプに分類し，骨化形態との相関を検討した。

（筆者ら作成）

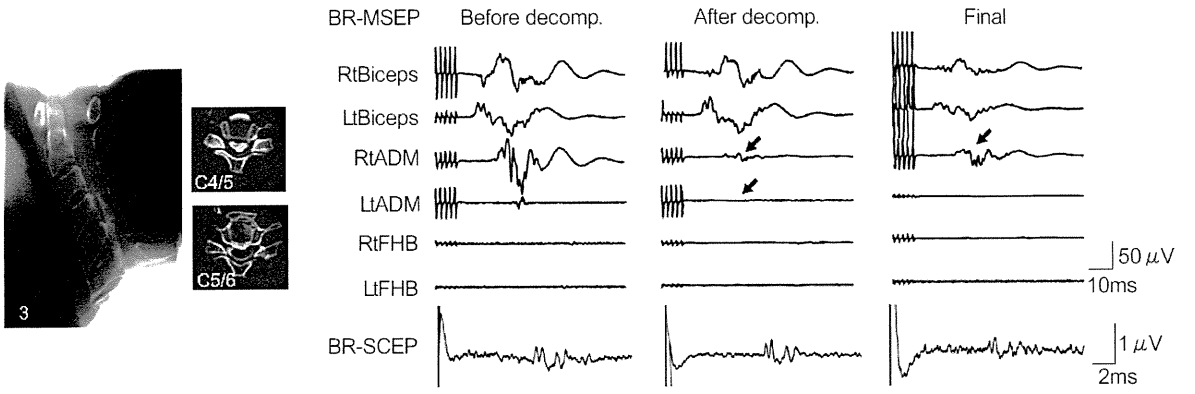

図5　症例3　58歳男性 C4-6 連続型 OPLL C3-7 前方除圧固定施行

骨化除圧直後に左ADM波形の消失。最狭窄部であるC5椎体の除圧が不十分と考え除圧を追加したが，手術終了時も振幅の改善は認められなかった。両FHBは手術開始時より導出が不良であったが，終了時左はほとんど消失している。術後，左上肢筋力低下と歩行障害が出現した。

（筆者ら作成）

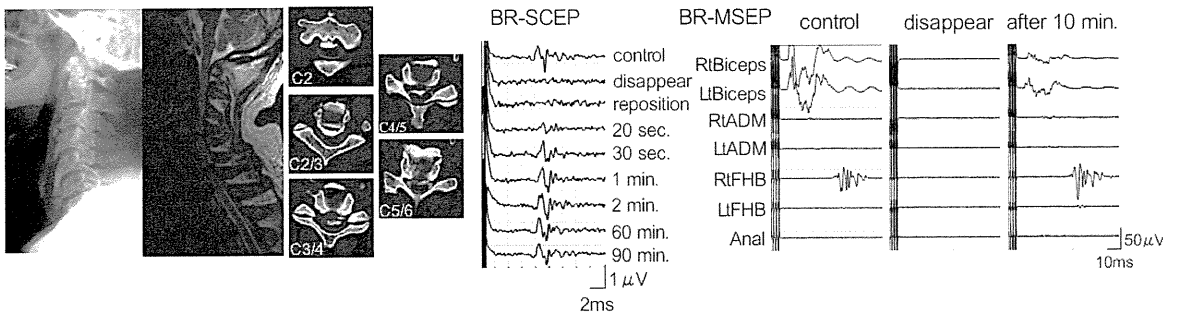

図6　症例4　64最男性 C2-6 混合型 OPLL 後方除圧術施行

椎弓展開時に脊髄誘発電位が消失。手術操作を休止し待機したが電位回復せず，8分後頸椎の屈曲姿位が原因であるが可能性を考えて，屈曲位から中間位へと矯正を行ったところ，直後から電位の回復を認めた。筋誘発電位も同様に，すべての筋電位が消失したが頸椎姿位矯正後電位の回復を認めた。術後に，脊髄障害を認めなかった。

（筆者ら作成）

により術者にアラームをだすことで，術後神経障害を回避したと思われる症例は5例あり，神経障害の原因は除圧操作2例，移植骨による頸椎伸長1例，頸椎姿位2例であった。アラームにより手術操作を休止し原因に対処することで術後神経障害は起こらなかった。術中モニタリングにより神経障害の原因が明らかになることは，手術手技の向上にもつながる。2004年以降，当施設でOPLL手術後の神経障害悪化は頸髄の片側の髄節障害1例のみであり，モニタリングにより手術の

BR-MSEP：経頭蓋電気刺激筋誘発電位

安全性が向上したことを特筆したい。

おわりに

OPLLは診断・手術ともに他疾患に比べ困難であることが多い。電気生理学的手法を駆使することで，OPLL診療の質を向上させることができる。

文　献

1) Shinomiya K, Furuya K, Yamaura I, et al：Spinal cord monitoring of spinal cord function using evoked spinal cord potentials, Fundamentals and clinical applications of spinal cord monitoring, ed by Homma S and Tamaki I, Saikon Publishing, Tokyo. p161-173, 1984.
2) Shinomiya K, Mochida K, Komori H, et al：Monitoring of Anterior Cervical Spinal Cord Function, Journal of Spinal Disorders **9**（3）：187-194, 1996.
3) K Shinomiya, K Furuya, R Satoh, et al：Electrophysiologic diagnosis of cervical OPLL myelopathy using evoked spinal cord potentials. Spine **13**：1225-1233, 1988.
4) 富澤將司，川端茂徳，新井嘉容ほか：脊髄誘発電位測定による頸椎後縦靱帯骨化症患者の脊髄障害高位診断：日本整形外科学会雑誌（0021-5325）**81**巻3号：S130, 2007.
5) 川端茂徳，富澤將司，四宮謙一ほか：術中脊髄モニタリングの有効性．臨床脳波（0485-1447）**51**巻5号：263-269, 2009.
6) 富澤將司，川端茂徳，新井嘉容ほか：頸椎後縦靱帯骨化症の術中脊髄モニタリング：日本整形外科学会雑誌（0021-5325）**81**巻3号:S130, 2007.

Biochemical and Biophysical Research Communications 383 (2009) 373–377

Contents lists available at ScienceDirect

Biochemical and Biophysical Research Communications

journal homepage: www.elsevier.com/locate/ybbrc

MCP-1 expressed by osteoclasts stimulates osteoclastogenesis in an autocrine/paracrine manner

Kana Miyamoto [a,b,c,*], Ken Ninomiya [a,c], Koh-Hei Sonoda [g], Yoshiteru Miyauchi [a,b], Hiroko Hoshi [a,b], Ryotaro Iwasaki [b,c,e], Hiroya Miyamoto [a,b], Shigeyuki Yoshida [b,e], Yuiko Sato [a,b], Hideo Morioka [a,b], Kazuhiro Chiba [a,b], Kensuke Egashira [h], Toshio Suda [c], Yoshiaki Toyama [a], Takeshi Miyamoto [a,b,c,d,f,i,*]

[a] Department of Orthopedic Surgery, Keio University School of Medicine, 35 Shinano-machi, Shinjuku-ku, Tokyo 160-8582, Japan
[b] Division of Orthopedic Research, Keio University School of Medicine, 35 Shinano-machi, Shinjuku-ku, Tokyo 160-8582, Japan
[c] Department of Cell Differentiation, The Sakaguchi Laboratory of Developmental Biology, Keio University School of Medicine, 35 Shinano-machi, Shinjuku-ku, Tokyo 160-8582, Japan
[d] Department of Musculoskeletal Reconstruction and Regeneration Surgery, Keio University School of Medicine, 35 Shinano-machi, Shinjuku-ku, Tokyo 160-8582, Japan
[e] Department of Dentistry and Oral Surgery, Keio University School of Medicine, 35 Shinano-machi, Shinjuku-ku, Tokyo 160-8582, Japan
[f] Kanrinmaru Project, Keio University School of Medicine, 35 Shinano-machi, Shinjuku-ku, Tokyo 160-8582, Japan
[g] Department of Ophthalmology, Graduate School of Medical Sciences, Kyushu University, 3-1-1, Maidashi, Higashi-ku, Fukuoka, Fukuoka 812-8582, Japan
[h] Department of Cardiovascular Medicine, Graduate School of Medical Sciences, Kyushu University, 3-1-1, Maidashi, Higashi-ku, Fukuoka, Fukuoka 812-8582, Japan
[i] Precursory Research for Embryonic Science and Technology, Japan Science and Technology Agency, Kawaguchi, Saitama 332-0012, Japan

ARTICLE INFO

Article history:
Received 3 April 2009
Available online 11 April 2009

Keywords:
Osteoclast
MCP-1
Autocrine/paracrine
DC-STAMP

ABSTRACT

Monocyte chemoattractant protein-1 (MCP-1) is a chemokine that plays a critical role in the recruitment and activation of leukocytes. Here, we describe that multinuclear osteoclast formation was significantly inhibited in cells derived from MCP-1-deficient mice. MCP-1 has been implicated in the regulation of osteoclast cell-cell fusion; however defects of multinuclear osteoclast formation in the cells from mice deficient in DC-STAMP, a seven transmembrane receptor essential for osteoclast cell-cell fusion, was not rescued by recombinant MCP-1. The lack of MCP-1 in osteoclasts resulted in a down-regulation of DC-STAMP, NFATc1, and cathepsin K, all of which were highly expressed in normal osteoclasts, suggesting that osteoclast differentiation was inhibited in MCP-1-deficient cells. MCP-1 alone did not induce osteoclastogenesis, however, the inhibition of osteoclastogenesis in MCP-1-deficient cells was restored by addition of recombinant MCP-1, indicating that osteoclastogenesis was regulated in an autocrine/paracrine manner by MCP-1 under the stimulation of RANKL in osteoclasts.

Osteoclasts are multinuclear cells derived from hematopoietic stem cells or monocyte/macrophage lineage cells [1]. Since osteoclasts are unique cells responsible for bone resorption, the control of osteoclast function or differentiation is critical to protect bones from bone diseases. Osteoclast formation is highly stimulated in destructive bone diseases such as rheumatoid arthritis (RA), multiple myeloma and bone metastasis [2–4]. Macrophage colony stimulating factor (M-CSF) and receptor activator of nuclear factor kappa B ligand (RANKL) have been reported to be expressed in osteoblast/stroma cells [5,6], and described to play a pivotal role in regulating osteoclastogenesis through their receptors, c-Fms and RANK, respectively, which are expressed in osteoclast progenitor cells [7–9]. Various factors such as vitamin D, PTHrP and PGE2 were reported to indirectly stimulate osteoclast differentiation through the upregulation of RANKL in osteoblast/stroma cells [6,10,11], however, the existence of an autocrine/paracrine system that stimulates osteoclastogenesis remains largely unclear.

Monocyte chemoattractant protein-1 (MCP-1)/Chemokine (C–C motif) ligand 2 (Ccl2) is a chemokine that belongs to the CC chemokine family and plays a critical role in the recruitment and activation of leukocytes during acute inflammation [12]. MCP-1 has been shown to play a critical role in the pathogenesis of arteriosclerosis and other vascular diseases by recruiting monocytes into the arterial wall [13]. MCP-1 has also been reported to be involved in osteoclast differentiation [14–17], however, studies of osteoclast differentiation using MCP-1-deficient mice have not been reported. Since MCP-1 has been implicated in the cell–cell fusion of osteoclasts [14–17], and MCP-1 family ligands share multiple receptors, it is possible that MCP-1 binds to an unknown receptor to stimulate osteoclast cell–cell fusion. Dendritic cell specific transmembrane receptor (DC-STAMP), an orphan seven transmembrane receptor, is essential for cell–cell fusion of osteoclasts, and DC-STAMP-deficient osteoclasts show a complete lack of cell–cell

* Corresponding authors. Address: Department of Orthopedic Surgery, Keio University School of Medicine, 35 Shinano-machi, Shinjuku-ku, Tokyo 160-8582, Japan. Fax: +81 3 3353 6597.
E-mail address: miyamoto@sc.itc.keio.ac.jp (T. Miyamoto).

0006-291X/$ - see front matter © 2009 Elsevier Inc. All rights reserved.
doi:10.1016/j.bbrc.2009.04.020

fusion [18–20]. DC-STAMP is highly induced in osteoclasts during differentiation [18,21] and is a direct target of NFATc1, an essential transcription factor for osteoclast differentiation [19,22]. Thus osteoclast differentiation and cell–cell fusion are both regulated by the RANKL-NFATc1 axis.

In this study, we describe that among MCP ligands, MCP-1 is specifically expressed in osteoclasts. MCP-1-deficient osteoclasts showed reduced multinuclear osteoclast differentiation and downregulation of NFATc1. Recombinant MCP-1 did not restore defective osteoclast cell–cell fusion in DC-STAMP-deficient cells. MCP-1 did not induced osteoclast differentiation in the absence of RANKL, whereas inhibited osteoclastogenesis in MCP-1-deficient cells was restored by recombinant MCP-1 in the presence of RANKL. Taken together, these findings suggest that MCP-1 expressed in osteoclasts plays a role in regulating osteoclast differentiation in an autocrine/paracrine manner under stimulation by RANKL.

Materials and methods

Mice. All animals were purchased from Japan Crea (Tokyo, Japan) or born and kept under pathogen-free conditions, and cared for in accordance with the guidelines of Keio University School of Medicine. *MCP-1*$^{-/-}$ mice were provided by Dr. Rollins ([23], Dana-Farber Cancer Institute, Boston, MA). *DC-STAMP*$^{-/-}$ mice were prepared as previously described [18,19].

Osteoclast differentiation in vitro. Bone marrow cells were isolated from *MCP-1*$^{-/-}$, *DC-STAMP*$^{-/-}$ or wild-type control mice and cultured in αMEM (Sigma–Aldrich, St. Louis, MO) medium containing 10% FCS in the presence of 50 ng/ml M-CSF (R&D, McKinley Place, MN, USA) at 37 °C in a humidified atmosphere of 5% CO_2 in air. After three days of culture, M-CSF-dependent adherent cells were harvested and cultured in the presence of M-CSF and RANKL (R&D) as previously described [18,19]. In some experiments, recombinant MCP-1 (R&D) was added to the culture. Osteoclastogenesis was evaluated by tartrate resistance acid phosphatase (TRAP) staining as described [24,25].

Microarray. Osteoclasts were formed from osteoclast progenitor cells isolated from wild-type mice, and total RNA was extracted. Oligonucleotide microarrays (GeneChip Mouse Genome 430 2.0 Array, Affymetrix) were used to monitor the relative abundance of transcripts.

Real-time Reverse Transcriptase-PCR. Total RNA was extracted from cultured osteoclasts using an RNeasy kit (Qiagen GmbH, Hilden, Germany), and cDNA was synthesized using the Advantage RT-for-PCR kit (Clontech, Mountain view, CA). *Cathepsin K, DC-STAMP* and *NFATc1* transcripts were quantified on ABI PRISM 7000 (Applied Biosystems, Foster City, USA) using TaqMan probes. *GAPDH* was used for sample normalization. Applied Biosystems assay IDs were Mm00484036_m1 (*Cathepsin K*), Mm01168058_m1 (*DC-STAMP*), Mm00479445_m1 (*NFATc1*), and 4352932E (*GAPDH*).

Statistical analysis. P values were calculated by the unpaired Student's *t*-test.

Results

MCP-1 is specifically expressed in osteoclasts and plays a critical role in osteoclastogenesis

The expression of the MCP ligands; MCP-1, 2, 3, and 4 were analyzed in murine osteoclasts by GeneChip analysis (Fig. 1A). MCP-1 was highly and specifically expressed in osteoclasts. This result led us to analyze the role of MCP-1 in osteoclastogenesis.

Osteoclast progenitor cells were isolated from MCP-1-deficient or wild-type mice, cultured in the presence of M-CSF and RANKL, and osteoclast differentiation was evaluated by TRAP staining and May-Gruenwald staining (Fig. 1B). Multinuclear osteoclast formation was significantly inhibited in MCP-1-deficient osteoclasts when compared to wild-type osteoclasts (Fig. 1B and C).

MCP-1 did not rescue the defective cell–cell fusion in DC-STAMP-deficient osteoclasts

Since MCP-1 was reportedly involved in osteoclast cell–cell fusion [14–17], MCP-1 was added to the culture to analyze whether it could rescue the inhibited cell-cell fusion of DC-STAMP-deficient osteoclasts (Fig. 2). However, the complete lack of cell–cell fusion in DC-STAMP-deficient osteoclasts was not restored by the addition of MCP-1 (Fig. 2A and B). MCP-1 did not induce cell–cell fusion or TRAP expression in wild-type cells in the absence of RANKL (Fig. 2A and B).

Osteoclast differentiation was inhibited in MCP-1-deficient cells

Since osteoclast cell–cell fusion is induced at the terminal stage of differentiation, the expression of *Cathepsin K* and *DC-STAMP*, a terminal differentiation marker for osteoclasts and an essential molecule for osteoclast cell–cell fusion, respectively, was analyzed

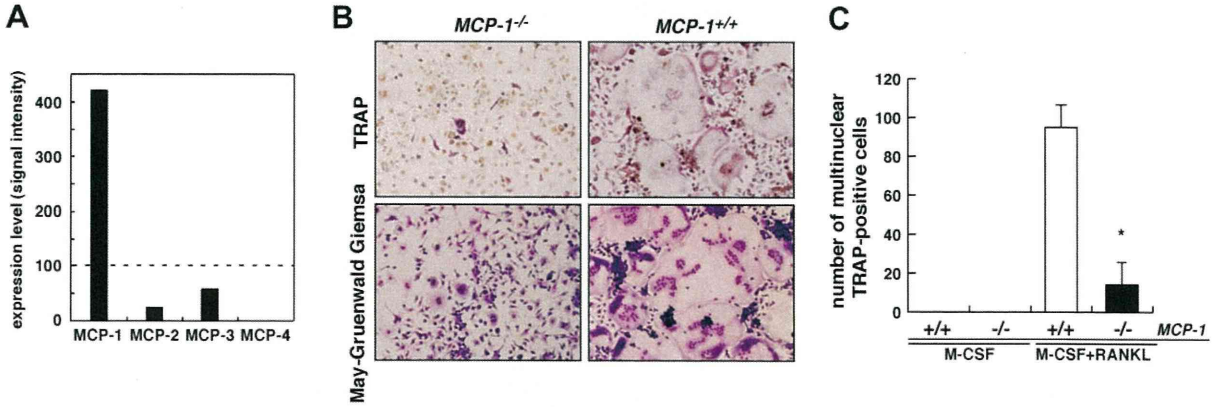

Fig. 1. MCP-1 expressed in osteoclasts plays a role in multinuclear osteoclast formation. (A) Osteoclasts were generated from wild-type osteoclast progenitor cells in the presence of M-CSF (50 ng/ml) and RANKL (25 ng/ml). RNA was extracted and GeneChip analysis was performed. Expression of MCP1, 2, 3, and 4 in osteoclasts is shown. MCP-1 is specifically expressed in osteoclasts. (B and C) Osteoclast progenitor cells were isolated from MCP-1-deficient (*MCP-1*$^{-/-}$) or wild-type (*MCP-1*$^{+/+}$) mice and cultured in the presence of M-CSF (50 ng/ml) and RANKL (25 ng/ml). After 7 days of culture, osteoclastogenesis was evaluated by TRAP staining (upper panel) or May-Gruenwald Giemsa staining (lower panel) (B), and the number of multinuclear TRAP-positive cells containing more than three nuclei was examined (C).

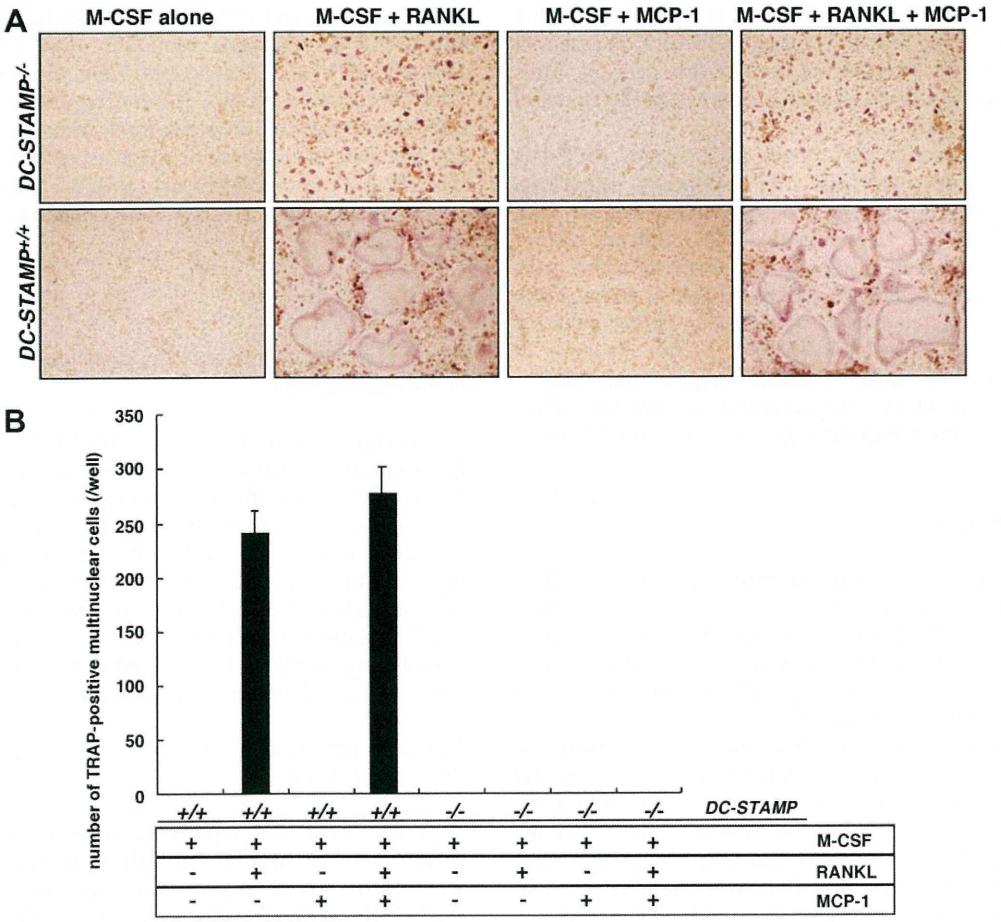

Fig. 2. MCP-1 does not function in DC-STAMP-deficient cells. Osteoclast progenitor cells were isolated from DC-STAMP-deficient (*DC-STAMP*$^{-/-}$) or wild-type (*DC-STAMP*$^{+/+}$) mice and cultured in the presence of M-CSF (50 ng/ml), M-CSF (50 ng/ml) + RANKL (25 ng/ml), M-CSF (50 ng/ml) + MCP-1 (100 ng/ml), and M-CSF (50 ng/ml) + RANKL (25 ng/ml) + MCP-1 (100 ng/ml). After 7 days of culture, osteoclastogenesis was evaluated by TRAP staining (A), and the number of multinuclear TRAP-positive cells containing more than three nuclei was scored (B).

(Fig. 3). *Cathepsin K* and *DC-STAMP* expression was significantly reduced in MCP-1-deficient osteoclasts compared to wild-type osteoclasts, indicating that osteoclastogenesis was inhibited in MCP-1-deficient osteoclasts. Since NFATc1 is an essential transcription factor for osteoclast differentiation and Cathepsin K and DC-STAMP are both direct targets of NFATc1 in osteoclasts [20,26], the expression of *NFATc1* was analyzed in MCP-1-deficient osteoclasts (Fig. 3). The expression of *NFATc1* was significantly downregulated in MCP-1-deficient osteoclasts compared with wild-type osteoclasts (Fig. 3), suggesting that MCP-1 expressed by osteoclasts induces osteoclast differentiation in an autocrine/paracrine manner.

MCP-1 plays a role in regulating osteoclastogenesis under stimulation by RANKL

In order to elucidate the role of MCP-1 in the regulation of osteoclast differentiation, recombinant MCP-1 was added to culture of MCP-1-deficient cells (Fig. 4). The inhibition of osteoclastogenesis seen in MCP-1-deficient cells was restored by the addition of MCP-1 in a dose-dependent manner, indicating that MCP-1 expressed in osteoclasts plays a critical role in regulating osteoclast differentiation. Osteoclast differentiation was not induced by MCP-1 in the absence of RANKL, suggesting that MCP-1 stimulates osteoclastogenesis under stimulation by RANKL (Fig. 4). Taken

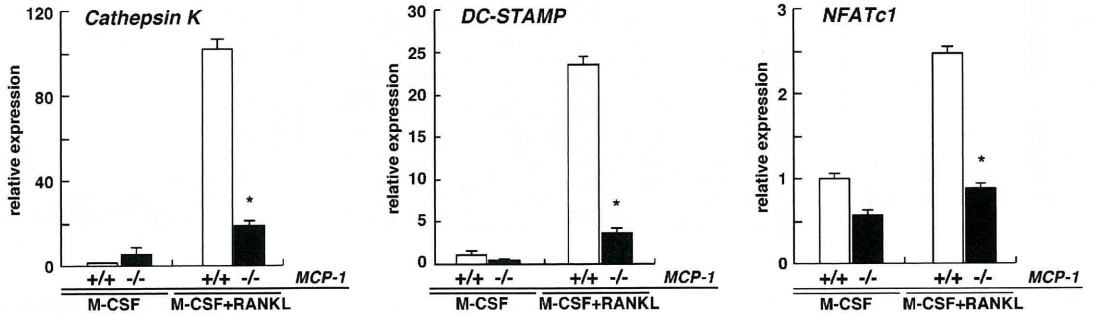

Fig. 3. Osteoclastogenesis is inhibited in MCP-1-deficient cells. Osteoclast progenitor cells were isolated from MCP-1-deficient (black column) or wild-type (white column) mice and cultured in the presence of M-CSF and RANKL. After 7 days of culture, total RNA was extracted, and real time PCR analysis was undertaken to determine the expression levels of indicated genes relative to *GAPDH* ($^{*}P < 0.01$).

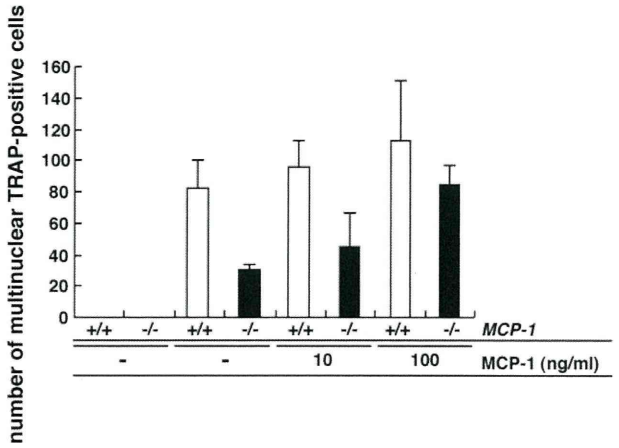

Fig. 4. Reduced osteoclastogenesis in MCP-1-deficient cells is restored by recombinant MCP-1. Osteoclast progenitor cells were isolated from MCP-1-deficient (black column) or wild-type (white column) mice and cultured in the presence of M-CSF (50 ng/ml) + RANKL (25 ng/ml) with or without the indicated concentrations of MCP-1. After 7 days of culture, osteoclastogenesis was evaluated by TRAP staining, and the number of multinuclear TRAP-positive cells containing more than three nuclei was scored.

together, our results indicate that MCP-1 expressed by osteoclasts plays a role in stimulating osteoclastogenesis induced by RANKL in an autocrine/paracrine manner.

Discussion

Osteoclastogenesis is induced by a combination of M-CSF and RANKL, both of which are cytokines expressed by osteoblasts, without osteoblasts/stromal cells [27]. The expression of RANKL in osteoblasts is upregulated by several factors such as vitamin D3 and PGE2 [6,10,11,27], and osteoclast differentiation has been considered to be controlled by microenvironmental factors [27]. The induction of osteoclastogenesis is simulated at sites of inflammation, bone metastasis and tooth eruption [2–4,28], suggesting that some factors may stimulate osteoclast differentiation at the site of bone destruction. In this study, we demonstrated that osteoclastogenesis induced by RANKL was further stimulated by MCP-1 expressed by osteoclasts in an autocrine/paracrine manner. MCP-1 expression has been detected at sites of RA, tooth eruption and bone metastasis where osteoclastogenesis is highly stimulated [29–32].

The most characteristic feature of osteoclasts is multinucleation induced by cell–cell fusion of mononuclear cells. We found that DC-STAMP was essential for cell–cell fusion of osteoclasts, and that osteoclast multinucleation was completely abrogated in DC-STAMP-deficient osteoclasts [18,19]. The multinucleation of osteoclasts through DC-STAMP upregulates their bone resorbing activity, suggesting that DC-STAMP is a molecule expressed by osteoclasts that stimulates osteoclast function [18]. Since DC-STAMP is an orphan receptor, a ligand that stimulates osteoclast cell-cell fusion and function may exist. DC-STAMP is a seven transmembrane receptor, and MCP-1 is known to bind to multiple receptors such as CCR2 and CCR11, both of which are seven transmembrane receptors. MCP-1 has been shown to induce differentiation and cell–cell fusion of osteoclasts [14–17,31], and DC-STAMP is reportedly involved in osteoclast differentiation [21].

Although its function was not demonstrated, MCP-1 expression in osteoclasts has previously been shown by large-scale expression analysis [33,34]. MCP-1 has been shown to induce differentiation without RANKL in human osteoclasts [14,15,31]. In our study, MCP-1 did not induce murine osteoclastogenesis without RANKL, suggesting that the differentiation system or requirement of MCP-1 for stimulating osteoclastogenesis is different between humans and mice; MCP-1 might be more critical for human osteoclastogenesis.

Our study establishes a function for MCP-1 expressed by osteoclasts on osteoclastogenesis. MCP-1 does not induce cell–cell fusion in DC-STAMP-deficient cells, but it plays a role in stimulating osteoclast differentiation under stimulation by RANKL in an autocrine/paracrine manner.

Acknowledgments

We thank B.J. Rollins for providing *MCP-1*$^{-/-}$ mice and Y. Sato for technical support. This work was supported by "High-Tech Research Center" Project for Private Universities: matching fund subsidy from MEXT (Ministry of Education, Culture, Sports, Science and Technology). T. Miyamoto was supported by a Grant-in-Aid for Young Scientists (B), Precursory Research for Embryonic Science and Technology, the JSPS Fujita Memorial Fund for Medical Research of Japan Society for the Promotion of Science, and a Grant-in-Aid from the Global COE Program of the Ministry of Education, Culture, Sports, Science and Technology, Japan, to Keio University.

References

[1] T. Miyamoto, T. Suda, Differentiation and function of osteoclasts, Keio J. Med. 52 (2003) 1–7.
[2] G. Schett, Cells of the synovium in rheumatoid arthritis. Osteoclasts, Arthritis Res. Ther. 9 (2007) 203.
[3] G.D. Roodman, Treatment strategies for bone disease, Bone Marrow Transplant. 40 (2007) 1139–1146.
[4] M. Cicek, M.J. Oursler, Breast cancer bone metastasis and current small therapeutics, Cancer Metastasis Rev. 25 (2006) 635–644.
[5] H. Yoshida, S. Hayashi, T. Kunisada, M. Ogawa, S. Nishikawa, H. Okamura, T. Sudo, L.D. Shultz, S. Nishikawa, The murine mutation osteopetrosis is in the coding region of the macrophage colony stimulating factor gene, Nature 345 (1990) 442–444.
[6] H. Yasuda, N. Shima, N. Nakagawa, K. Yamaguchi, M. Kinosaki, S. Mochizuki, A. Tomoyasu, K. Yano, M. Goto, A. Murakami, E. Tsuda, T. Morinaga, K. Higashio, N. Udagawa, N. Takahashi, T. Suda, Osteoclast differentiation factor is a ligand for osteoprotegerin/osteoclastogenesis-inhibitory factor and is identical to TRANCE/RANKL, Proc. Natl. Acad. Sci. USA 95 (1998) 3597–3602.
[7] F. Arai, T. Miyamoto, O. Ohneda, T. Inada, T. Sudo, K. Brasel, T. Miyata, D.M. Anderson, T. Suda, Commitment and differentiation of osteoclast precursor cells by the sequential expression of c-Fms and receptor activator of nuclear factor kappaB (RANK) receptors, J. Exp. Med. 190 (1999) 1741–1754.
[8] Y.Y. Kong, H. Yoshida, I. Sarosi, H.L. Tan, E. Timms, C. Capparelli, S. Morony, A.J. Oliveira-dos-Santos, G. Van, A. Itie, W. Khoo, A. Wakeham, C.R. Dunstan, D.L. Lacey, T.W. Mak, W.J. Boyle, J.M. Penninger, OPGL is a key regulator of osteoclastogenesis, lymphocyte development and lymph-node organogenesis, Nature 397 (1999) 315–323.
[9] W.C. Dougall, M. Glaccum, K. Charrier, K. Rohrbach, K. Brasel, T. De Smedt, E. Daro, J. Smith, M.E. Tometsko, C.R. Maliszewski, A. Armstrong, V. Shen, S. Bain, D. Cosman, D. Anderson, P.J. Morrissey, J.J. Peschon, J. Schuh, RANK is essential for osteoclast and lymph node development, Genes Dev. 13 (1999) 2412–2424.
[10] R.J. Thomas, T.A. Guise, J.J. Yin, J. Elliott, N.J. Horwood, T.J. Martin, M.T. Gillespie, Breast cancer cells interact with osteoblasts to support osteoclast formation, Endocrinology 140 (1999) 4451–4458.
[11] M. Nagai, N. Sato, Reciprocal gene expression of osteoclastogenesis inhibitory factor and osteoclast differentiation factor regulates osteoclast formation, Biochem. Biophys. Res. Commun. 257 (1999) 719–723.
[12] R.K. Tangirala, K. Murao, O. Quehenberger, Regulation of expression of the human monocyte chemotactic protein-1 receptor (hCCR2) by cytokines, J. Biol. Chem. 272 (1997) 8050–8056.
[13] S. Kitamoto, K. Egashira, Gene therapy targeting monocyte chemoattractant protein-1 for vascular disease, J. Atheroscler. Thromb. 9 (2002) 261–265.
[14] M.S. Kim, C.J. Day, N.A. Morrison, MCP-1 is induced by receptor activator of nuclear factor-{kappa}B ligand, promotes human osteoclast fusion, and rescues granulocyte macrophage colony-stimulating factor suppression of osteoclast formation, J. Biol. Chem. 280 (2005) 16163–16169.
[15] M.S. Kim, C.J. Day, C.I. Selinger, C.L. Magno, S.R. Stephens, N.A. Morrison, MCP-1-induced human osteoclast-like cells are tartrate-resistant acid phosphatase, NFATc1, and calcitonin receptor-positive but require receptor activator of NFkappaB ligand for bone resorption, J. Biol. Chem. 281 (2006) 1274–1285.
[16] X. Li, L. Qin, M. Bergenstock, L.M. Bevelock, D.V. Novack, N.C. Partridge, Parathyroid hormone stimulates osteoblastic expression of MCP-1 to recruit and increase the fusion of pre/osteoclasts, J. Biol. Chem. 282 (2007) 33098–33106.

[17] H. Hounoki, E. Sugiyama, S.G. Mohamed, K. Shinoda, H. Taki, H.O. Abdel-Aziz, M. Maruyama, M. Kobayashi, T. Miyahara, Activation of peroxisome proliferator-activated receptor gamma inhibits TNF-alpha-mediated osteoclast differentiation in human peripheral monocytes in part via suppression of monocyte chemoattractant protein-1 expression, Bone 42 (2008) 765–774.
[18] M. Yagi, T. Miyamoto, Y. Sawatani, K. Iwamoto, N. Hosogane, N. Fujita, K. Morita, K. Ninomiya, T. Suzuki, K. Miyamoto, Y. Oike, M. Takeya, Y. Toyama, T. Suda, DC-STAMP is essential for cell-cell fusion in osteoclasts and foreign body giant cells, J. Exp. Med. 202 (2005) 345–351.
[19] M. Yagi, K. Ninomiya, N. Fujita, T. Suzuki, R. Iwasaki, K. Morita, N. Hosogane, K. Matsuo, Y. Toyama, T. Suda, T. Miyamoto, Induction of DC-STAMP by alternative activation and downstream signaling mechanisms, J. Bone Miner. Res. 22 (2007) 992–1001.
[20] T. Miyamoto, The dendritic cell-specific transmembrane protein DC-STAMP is essential for osteoclast fusion and osteoclast bone-resorbing activity, Mod. Rheumatol. 16 (2006) 341–342.
[21] T. Kukita, N. Wada, A. Kukita, T. Kakimoto, F. Sandra, K. Toh, K. Nagata, T. Iijima, M. Horiuchi, H. Matsusaki, K. Hieshima, O. Yoshie, H. Nomiyama, RANKL-induced DC-STAMP is essential for osteoclastogenesis, J. Exp. Med. 200 (2004) 941–946.
[22] K. Kim, S.H. Lee, J. Ha Kim, Y. Choi, N. Kim, NFATc1 induces osteoclast fusion via up-regulation of Atp6v0d2 and the dendritic cell-specific transmembrane protein (DC-STAMP), Mol. Endocrinol. 22 (2008) 176–185.
[23] B. Lu, B.J. Rutledge, L. Gu, J. Fiorillo, N.W. Lukacs, S.L. Kunkel, R. North, C. Gerard, B.J. Rollins, Abnormalities in monocyte recruitment and cytokine expression in monocyte chemoattractant protein 1-deficient mice, J. Exp. Med. 187 (1998) 601–608.
[24] T. Miyamoto, F. Arai, O. Ohneda, K. Takagi, D.M. Anderson, T. Suda, An adherent condition is required for formation of multinuclear osteoclasts in the presence of macrophage colony-stimulating factor and receptor activator of nuclear factor kappa B ligand, Blood 96 (2000) 4335–4343.
[25] T. Miyamoto, O. Ohneda, F. Arai, K. Iwamoto, S. Okada, K. Takagi, D.M. Anderson, T. Suda, Bifurcation of osteoclasts and dendritic cells from common progenitors, Blood 98 (2001) 2544–2554.
[26] M. Matsumoto, M. Kogawa, S. Wada, H. Takayanagi, M. Tsujimoto, S. Katayama, K. Hisatake, Y. Nogi, Essential role of p38 mitogen-activated protein kinase in cathepsin K gene expression during osteoclastogenesis through association of NFATc1 and PU.1, J. Biol. Chem. 279 (2004) 45969–45979.
[27] T. Suda, N. Takahashi, N. Udagawa, E. Jimi, M.T. Gillespie, T.J. Martin, Modulation of osteoclast differentiation and function by the new members of the tumor necrosis factor receptor and ligand families, Endocr. Rev. 20 (1999) 345–357.
[28] M. Yoshino, H. Yamazaki, H. Yoshida, S. Niida, S. Nishikawa, K. Ryoke, T. Kunisada, S. Hayashi, Reduction of osteoclasts in a critical embryonic period is essential for inhibition of mouse tooth eruption, J. Bone Miner. Res. 18 (2003) 108–116.
[29] A.E. Koch, S.L. Kunkel, L.A. Harlow, B. Johnson, H.L. Evanoff, G.K. Haines, M.D. Burdick, R.M. Pope, R.M. Strieter, Enhanced production of monocyte chemoattractant protein-1 in rheumatoid arthritis, J. Clin. Invest. 90 (1992) 772–779.
[30] G.E. Wise, S. Frazier-Bowers, R.N. D'Souza, Cellular, molecular, and genetic determinants of tooth eruption, Crit. Rev. Oral Biol. Med. 13 (2002) 323–334.
[31] Y. Lu, Z. Cai, G. Xiao, E.T. Keller, A. Mizokami, Z. Yao, G.D. Roodman, J. Zhang, Monocyte chemotactic protein-1 mediates prostate cancer-induced bone resorption, Cancer Res. 67 (2007) 3646–3653.
[32] R. Aggarwal, I.M. Ghobrial, G.D. Roodman, Chemokines in multiple myeloma, Exp. Hematol. 34 (2006) 1289–1295.
[33] D. Cappellen, N.H. Luong-Nguyen, S. Bongiovanni, O. Grenet, C. Wanke, M. Susa, Transcriptional program of mouse osteoclast differentiation governed by the macrophage colony-stimulating factor and the ligand for the receptor activator of NFkappa B, J. Biol. Chem. 277 (2002) 21971–21982.
[34] N. Ishida, K. Hayashi, M. Hoshijima, T. Ogawa, S. Koga, Y. Miyatake, M. Kumegawa, T. Kimura, T. Takeya, Large scale gene expression analysis of osteoclastogenesis in vitro and elucidation of NFAT2 as a key regulator, J. Biol. Chem. 277 (2002) 41147–41156.

SPINE Volume 34, Number 24, pp E882–E885

Primary NK/T-Cell Lymphoma of the *Cauda Equina*

A Case Report and Literature Review

Masahiro Morita, MD,* Masahiko Osawa, MD, PhD,† Hirotsune Naruse, MD, PhD,‡ and Hiroaki Nakamura, MD, PhD§

Study Design. A case report with a review of the literature.

Objective. To describe an unusual case of primary lymphoma of the *cauda equina* and provide a review of the literature of this condition.

Summary of Background Data. Primary lymphoma of the cauda equina is extremely rare, and has been reported in 8 cases previously. This report is the first to describe a case of primary nasal type NK/T-cell lymphoma of the *cauda equina.*

Methods. We report the case of a 67-year-old man presenting the symptoms of cauda equina syndrome caused by primary lymphoma of the *cauda equina.*

Results. After laminectomy and removal of the tumor, the patient recovered from the symptoms of cauda equina syndrome except for bladder and bowel dysfunction. Further investigations including immunohistochemical stains made a diagnosis of primary nasal type NK/T-cell lymphoma of the *cauda equina,* and the patient received radiotherapy to the lumbosacral area. Brain metastasis was detected 8 months after surgery, and the patient died 14 months after his initial clinical presentation despite additional treatments including whole-brain radiotherapy and oral chemotherapy.

Conclusion. Although primary lymphoma of the cauda equina is extremely rare, the prognosis of this condition is thought to be poor. Early definitive diagnosis with examination of the cerebrospinal fluid followed by combined treatment with radiotherapy and high-dose methotrexate should be considered.

Key words: primary lymphoma, nasal type NK/T-cell lymphoma, *cauda equina.* **Spine 2009;34:E882–E885**

Spinal involvement is not uncommon in the advanced stage of malignant lymphoma. However, primary lymphoma of the spine has been reported to account for about one-third of all primary bone lymphomas which accounts for <5% of extranodal lymphomas and <2% of all lymphomas in adults.[1] Clinical manifestations of the disease may vary, and they may include back pain due to pathologic fractures, as well as leg symptoms, such as leg pain or motor weakness due to spinal cord compression. Spinal epidural involvement has been reported in 0.8% to 2.8% of all malignant lymphoma cases.[2]

On the other hand, primary central nervous system lymphoma is also an extranodal non-Hodgkin lymphoma that arises from the brain parenchyma, eyes, meninges, or spinal cord in the absence of systemic disease; the spinal cord is the rarest site of involvement in patients with this condition.[3] In addition, primary lymphoma of the *cauda equina* is extremely rare. The purpose of this article is to describe the detailed clinical and pathologic findings of an extremely rare case of nasal type NK/T-cell lymphoma that had a primary origin from the *cauda equina* with a review of the literature.

■ Case Report

A 67-year-old man was referred to our hospital with a 2-month history of severe leg pain as well as bladder and bowel dysfunction. The symptoms had progressed within a few weeks after onset, and he could not walk because of severe leg pain. Before the onset of symptoms, he had been in good general health. Physical examination revealed mild motor weakness in both lower extremities, predominantly affecting the distal muscles, bilateral absence of lower limb reflexes, and severe diminished pinprick and light touch sensation in his perineal region despite almost normal neurologic findings in his upper extremities and normal cranial nerve function. Routine hematological and biochemical tests, as well as Human Immunodeficiency virus serology, were normal. Magnetic resonance imaging of his lumbar spine revealed spinal canal stenosis at L4/5 and a mass lesion with an apparent intensity change occupying nearly the entire thecal sac from L3–L5, with nonmarked demarcation to the normal *cauda equina.* The mass had marked and homogeneous enhancement after intravenous injection of gadolinium-DTPA. A lumbar myelogram demonstrated complete block of the contrast medium at L3/4 (Figure 1). Magnetic resonance imaging of his brain and total spine revealed no evidence of other involvement. After bilateral laminectomy at L3–L5 and incision of the dural sac, the *cauda equina* was noted to be swollen and reddish-gray tumors were present. The tumors infiltrated extensively between the *cauda equina* and adhered strongly to the nerve root. The tumors were removed as far as possible with special attention not to damage the nerve root. After surgery, the patient's severe leg pain improved considerably, and he could walk without a cane or a walker, but bladder and bowel dysfunction still

From the *Department of Orthopaedic Surgery, Izumi Municipal Hospital, Izumi City, Osaka, Japan; †Department of Diagnostic Pathology, Osaka City University Graduate School of Medicine, Abeno, Osaka, Japan; ‡Department of Neurosurgery, Izumi Municipal Hospital, Izumi City, Osaka, Japan; and §Department of Orthopaedic Surgery, Osaka City University Graduate School of Medicine, Abeno, Osaka, Japan.

Acknowledgment date: November 23, 2008. First revision date: March 12, 2009. Acceptance date: April 6, 2009.

The manuscript submitted does not contain information about medical device(s)/drug(s).

No funds were received in support of this work. No benefits in any form have been or will be received from a commercial party related directly or indirectly to the subject of this manuscript.

Address correspondence and reprint requests to Masahiro Morita, MD, Department of Orthopaedic Surgery, Izumi Municipal Hospital, 4–10–10 Fuchu Izumi City Osaka, 594–0071, Japan; E-mail: m1908130@msic.med.osaka-cu.ac.jp

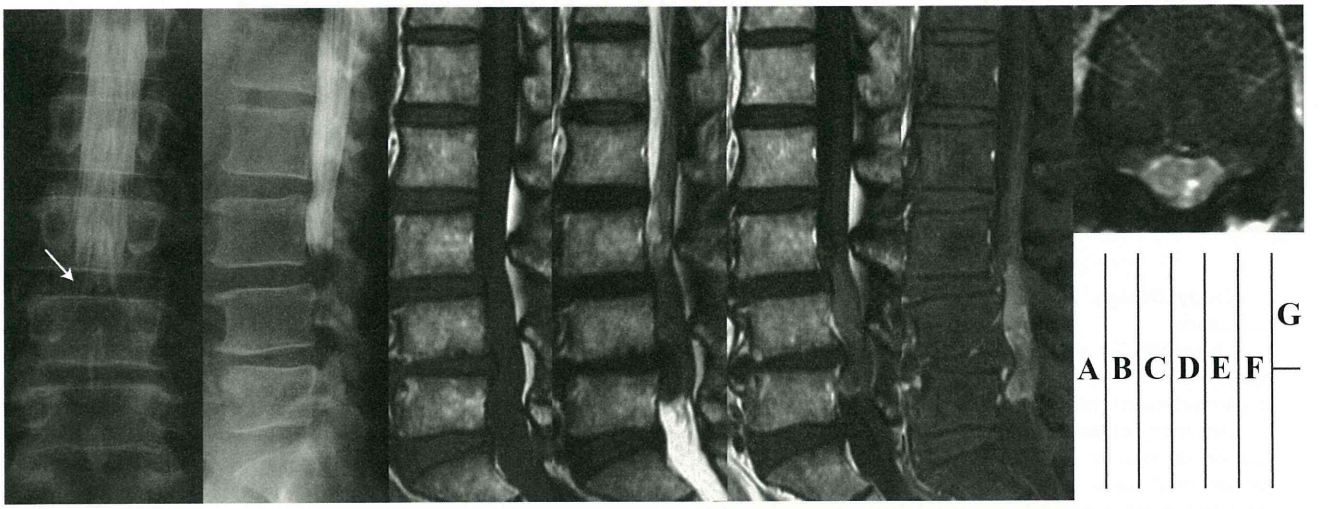

Figure 1. Myelography—(**A**) posteroanterior, (**B**) lateral—showing a complete block at L3/4, and nodular thickening of the lumbar nerve roots (arrow). Magnetic resonance imaging—(**C**) T1-weighted sagittal image, (**D**) T2-weighted sagittal image, (**E**) T1-weighted sagittal image with gadolinium enhancement, (**F**) T1-weighted and fat suppression sagittal image with gadolinium enhancement, (**G**) T1-weighted and fat suppression axial image with gadolinium enhancement at L4—showing an intrathecal mass at the lesion and marked enhancement with gadolinium.

remained. A diagnosis of nasal type NK/T-cell lymphoma of the *cauda equina* was made based on immunohistochemical stains. Further investigations, including gallium and technetium scintigraphy, thoracic, abdominal, and pelvic computed tomography, and bone marrow biopsy of the iliac bone, did not reveal any other site of lymphoma. The patient received radiotherapy to the lumbosacral area with a dose of 50 Gy after surgery but refused chemotherapy. A routine metastatic workup demonstrated unremarkable findings until he complained of clouding of consciousness, which was caused by brain metastasis 8 months after surgery. Despite whole-brain radiotherapy (30 Gy) and oral chemotherapy (etoposide), the patient died 14 months after his initial clinical presentation.

■ Pathologic Findings

The medium-sized and large-sized lymphoid cells with irregular nuclei showed diffuse proliferation among the necrotic nerve fibers in the *cauda equina* (Figure 2). Coagulative necrosis and angiocentric infiltration of lymphoma cells were also found in the tumor. The inflammatory cells, including neutrophils, macrophages, plasma cells, and eosinophils, were also intermingled. On immunohistochemistry, the lymphoma cells were positive for CD3 and CD56, detected by immunohistochemical method using monoclonal antibodies, anti-CD3 (PS1, Immunotech, Marseilla, France) and anti-CD56 (1B6, Nichirei Bioscience, Tokyo, Japan). Epstein Barr viral early RNA-1 was detected in the nucleus of the lymphoma cells by *in situ* hybridization, using the Epstein Barr viral early RNA-1 probe.

■ Discussion

Primary central nervous system lymphoma is an extranodal non-Hodgkin lymphoma that accounts for 5% to 7% of primary brain tumors and 1% to 2% of all cases of non-Hodgkin lymphoma.[4] The spinal cord is the rarest site of involvement in patients with primary central nervous system lymphoma, although meningeal dissem-

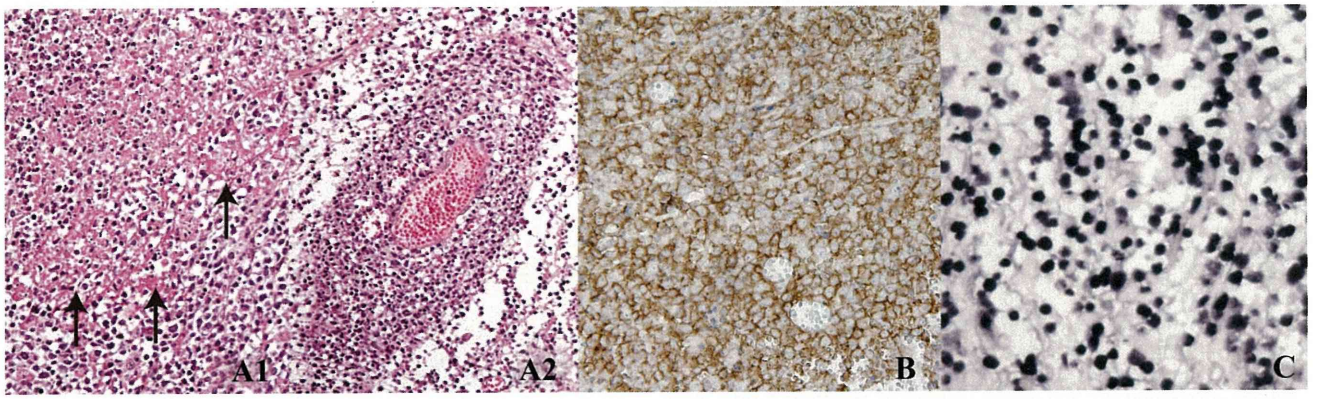

Figure 2. Diffuse proliferation of lymphoma cells with the coagulative necrosis of lymphoma cells (arrow) (**A-1**) and angiocentric pattern of lymphoid (**A-2**) infiltrate in the fascia of the cauda equina (hematoxylin-eosin stain). **B,** Lymphoma cells are positive for CD56. **C,** Epstein Barr virus was detected in the nucleus of lymphoma cells by Epstein Barr viral early RNA *in situ* hybridization. Magnification, ×350.

Table 1. Literature Review of Patients With Primary Lymphoma of the *Cauda Equina*

Reference	Age/Sex	Interval (Onset-Diagnosis)	Pathology	Treatment	Outcome	F/U
Mauney and Sciotto[6]	68/F	1 wk	B cell lymphoma	RT	Alive	3 mo
Toner *et al*[7]	59/M	3 mo	B cell lymphoma	RT, CT (Intrathecal and intravenous)	Alive	2 yr
Klein *et al*[8]	29/F	2 wk	B cell lymphoma	N.A.	Died	5 wk
Knopp *et al*[9]	69/F	3 wk	N.A.	N.A.	N.A.	N.A.
Ooi *et al*[10]	16/M	3 wk	T-lymphoblastic lymphoma	RT, CT (Intrathecal and intravenous)	Died	8 mo
Giobbia *et al*[11]	30/F	2 mo	B cell lymphoma	RT, CT (Intrathecal)	Alive	1 yr
Zagami and Granot[12]	71/F	3 wk	B cell lymphoma	CT (Intrathecal)	Died	16 mo
Tajima *et al*[13]	67/F	3 yr	B cell lymphoma	RT, CT (Intrathecal)	Alive	3 yr

N.A. indicates not available; RT, radiation therapy; CT, chemotherapy; F/U, duration of follow-up after onset.

ination to the spinal cord from an intracranial focus may sometimes occur at an advanced stage of systemic lymphoma. Although previous studies report that less than 1% of primary central nervous system lymphoma occur in the spinal cord,[5] the rate of primary lymphoma in the *cauda equina* has not been reported.

Based on our review of the English literature[6–13] (Table 1), only 8 cases of primary lymphoma of the *cauda equina* have been reported. A summary of the clinical course, imaging findings, and histologic findings of these reports is presented.

First, the symptoms of *cauda equina* syndrome, such as lower extremity paresthesia, muscular weakness, and bladder dysfunction, progress rapidly within a short period of time. Most cases, including the present case, presented with a few weeks history of progressive symptoms. Second, the *cauda equina* lesions show isointense or increased signals on T1-weighted magnetic resonance images and increased signals on T2-weighted images, along with no abnormal signal changes in the vertebrae. However, marked enhancement of the *cauda equina* lesions on gadolinium-DTPA-enhanced T1-weighted images is observed, which can be useful for identifying the lesions. A thickened *cauda equina* nerve root on magnetic resonance imaging after gadolinium-DTPA enhancement[8,12,13] or on myelography[7,8] is another imaging finding. Lastly, although Ooi *et al*[10] reported T-lymphoblastic primary lymphoma of the *cauda equina*, primary lymphoma of the *cauda equina* is predominantly non-Hodgkin lymphoma of the B-cell type.

The differential diagnosis of primary intradural tumors arising at the level of *cauda equina* (including conus region) consists mainly of neurofibromas, ependymomas, and schwannomas, and less commonly meningiomas, dermoids, epidermoids, paragangliomas, high grade gliomas, hemangioblastomas, and so on.[14]

Magnetic resonance imaging using gadolinium enhancement can usually suggest the nature of the tumor. Almost all tumors enhance, and gadolinium helps to separate the solid portion of tumors from adjacent edema and associated cysts.[15] Schwannomas demonstrate isointence on T1-weighted and hyperintence on T2-weighted magnetic resonance images, and usually have more irregular enhancement in comparison to meningiomas because of internal necrosis and/or cystic degeneration. Meningiomas demonstrate isointence on both T1- and T2- weighted magnetic resonance images and hyperintence on contrast enhanced, and ependymomas, which almost exclusively have a myxopathic histology at this level, demonstrate isointence on T1- weighted and hyperintence on T2-weighted magnetic resonance images and contrast enhanced.[14]

Other than open biopsy, definitive diagnosis using a cytocentrifuge preparation of the cerebrospinal fluid has been suggested; some authors have recommended routine cerebrospinal fluid evaluation.[6,16]

Optimal treatment for primary central nervous system lymphoma, which was previously treated with radiotherapy alone,[17] has not yet been established.[18] On the other hand, there are convincing data that high-dose methotrexate-based chemotherapy regimens provide better survival rates than radiotherapy alone.[19] However, the rates of permanent neurologic side effects following combined treatment with radiotherapy and high-dose methotrexate are unacceptably high in the elderly population.[17] As described in the present case report, primary lymphoma of the *cauda equina* should be differentiated even if there is no spinal involvement. As the prognosis with this lesion is not good, early definitive diagnosis with examination of the cerebrospinal fluid followed by combined treatment with radiotherapy and high-dose methotrexate should be considered.

■ Key Points

- The first case of primary nasal type NK/T-cell lymphoma of the *cauda equina* is reported.
- Optimal treatment for primary lymphoma of the *cauda equina* has not yet been established, and the prognosis of this condition is thought to be poor.
- Early definitive diagnosis with examination of the cerebrospinal fluid followed by combined treatment with radiotherapy and high-dose methotrexate should be considered.

References

1. Ramadan KM, Shenkier T, Sehn LH, et al. A clinicopathological retrospective study of 131 patients with primary bone lymphoma: a population-based

study of successively treated cohorts from the British Columbia Cancer Agency. *Ann Oncol* 2007;18:129–35.
2. Székely G, Miltényi Z, Mezey G, et al. Epidural malignant lymphomas of the spine: collected experiences with epidural malignant lymphomas of the spinal canal and their treatment. *Spinal Cord* 2008;46:278–81.
3. Eichler AF, Batchelor TT. Primary central nervous system lymphoma: presentation, diagnosis and staging. *Neurosurg Focus* 2006;21:1–9.
4. Iwamoto FM, DeAngelis LM. An update on primary central nervous system lymphoma. *Hematol Oncol Clin North Am* 2006;20:1267–85.
5. Hochberg FH, Miller DC. Primary central nervous system lymphoma. *J Neurosurg* 1988;68:835–53.
6. Mauney M, Sciotto CG. Primary malignant lymphoma of the cauda equina. *Am J Surg Pathol* 1983;7:185–190.
7. Toner GC, Holmes R, Sinclair RA, et al. Central nervous system lymphoma: primary lumber nerve root infiltration. *Acta Haematol* 1989;81:44–7.
8. Klein P, Zientek G, Vandenberg SR, et al. Primary CNS lymphoma: lymphomatous meningitis presenting as a cauda equina lesion in an AIDS patient. *Can J Neurol Sci* 1990;17:329–31.
9. Knopp EA, Chynn KY, Hughes J. Primary lymphoma of the cauda equina: myelographic, CT myelographic, and MR appearance. *AJNR Am J Neuroradiol* 1994;15:1187–9.
10. Ooi GC, Peh WC, Fung CF. Case report: magnetic resonance imaging of primary lymphoma of the cauda equina. *Br J Radiol* 1996;69:1057–60.
11. Giobbia M, Carniato A, Scotton PG, et al. Primary EBV-associated cauda equina lymphoma. *J Neurol* 1999;246:739–40.
12. Zagami AS, Granot R. Non-Hodgkin's lymphoma involving the cauda equina and ocular cranial nerves: case reports and literature review. *J Clin Neurosci* 2003;10:696–9.
13. Tajima Y, Sudo K, Matumoto A. Malignant lymphoma originating in the cauda equina mimicking the inflammatory polyradiculoneuropathy. *Intern Med* 2007;46:1029–32.
14. Kotil T, Bilge T. Primary intradural conus and cauda equina tumors: long-time outcome with 14 years follow-up. *Turkish Neurosurgery* 2006;16:130–8.
15. Mathew P, Todd NV. Intradural conus and cauda equina tumours: a retrospective review of presentation, diagnosis and early outcome. *J Neurol Neurosurg Psychiatry* 1993;56:69–74.
16. MacKintosh FR, Colby TV, Podolsky WJ, et al. Central nervous system involvement in non-Hodgkin's lymphoma: an analysis of 105 cases. *Cancer* 1982;49:586–95.
17. DeAngelis LM, Iwamoto FM. An update on therapy of primary central nervous system lymphoma. *Hematology Am Soc Hematol Educ Program* 2006;311–6.
18. Yamanaka R, Morii K, Shinbo Y, et al. Results of treatment of 112 cases of primary CNS lymphoma. *Jpn J Clin Oncol* 2008;38:373–80.
19. Ferreri AJ, Abrey LE, Blay JY, et al. Summary statement on primary central nervous system lymphoma from the Eighth International Conference on malignant lymphoma, Lugano, Switzerland, June 12 to 15, 2002. *J Clin Oncol* 2003;21:2407–14.

Clin Orthop Relat Res (2009) 467:3206–3212
DOI 10.1007/s11999-009-0960-1

SYMPOSIUM: TRIBUTE TO DR. MARSHALL URIST: MUSCULOSKELETAL GROWTH FACTORS

Successful Spinal Fusion by E. coli-derived BMP-2-adsorbed Porous β-TCP Granules

A Pilot Study

**Sho Dohzono MD, Yuuki Imai MD, PhD,
Hiroaki Nakamura MD, PhD, Shigeyuki Wakitani MD, PhD,
Kunio Takaoka MD, PhD**

Published online: 7 July 2009

Abstract Bone morphogenetic proteins (BMPs) were originally identified as osteoinductive proteins. With cloning of BMP genes, studies of BMPs and their clinical application have advanced. However, with increasing clinical applications, drug delivery systems and production costs have become more important issues. To address these issues, we asked whether E. coli-derived rhBMP-2 (E-BMP-2)-adsorbed porous β-TCP granules could achieve posterolateral lumbar fusion in a rabbit model similar to autogenous bone grafts. Lumbar spinal fusion masses were evaluated by 3-D computed tomography, mechanical testing, and histological analyses 8 weeks after surgery. By these measures E-BMP-2-adsorbed β-TCP granules achieved lumbar spinal fusion in dose-dependent fashion in a rabbit model as well as autogenous bone graft. Our preliminary findings suggest E-BMP-2-adsorbed porous β-TCP could be a novel, effective alternative to autogenous bone grafting for generating new bone and promoting regenerative repair of bone, and potentially utilizable in the clinical setting for treating spinal disorders.

Each author certifies that he or she has no commercial associations (eg, consultancies, stock ownership, equity interest, patent/licensing arrangements, etc) that might pose a conflict of interest in connection with the submitted article. This work was supported in part by Grants-in-Aid from the Ministry of Education, Culture, Sports, Science, and Technology of Japan (Project Grants 16109009 and 1679085 to KT, and 19791018 to YI).
Each author certifies that his or her institution has approved the animal protocol for this investigation and that all investigations were conducted in conformity with ethical principles of research.

S. Dohzono, Y. Imai (✉), H. Nakamura, S. Wakitani, K. Takaoka
Department of Orthopaedic Surgery, Osaka City University Graduate School of Medicine, 1-4-3 Asahimachi, Abeno-ku, Osaka, Osaka 545-8585, Japan
e-mail: imai@med.osaka-cu.ac.jp

Introduction

Autogenous bone grafting from the iliac bone has commonly been used clinically to promote bone formation, such as in fusion of the unstable spine, repair of large bone defects, and treatment of pseudarthrosis. However, autogenous bone grafting has several disadvantages, including acute and/or chronic pain or dysesthesia, potential risk of wound infection, unsightly scars, and deformity at the donor site [4, 19]. Limited available mass of graft bone is an additional disadvantage, especially in cases of large augmentation and long fusion after correction of scoliosis. To avoid these problems various authors have proposed new materials or agents that can substitute for autogenous bone grafts, such as bioabsorbable polymers, hyaluronic acid, and others [3, 30, 35].

The use of BMPs with their osteoinductive properties [39] has long been considered a promising means of producing such bone graft substitutes. This concept, however, was practically realized after successful cloning of cDNAs of BMPs [42]. Recombinant BMPs (BMP-2 and BMP-7) are currently utilized in combination with bovine collagen carrier in clinical practice to treat skeletal disorders such as open fracture, anterior interbody fusion, and posterolateral lumbar fusion [1, 2, 5–11, 13–17, 20, 22, 23, 25, 26, 31, 34, 41]. However, problems remain with the use of animal-derived collagen, including the risk of generation of antibody or disease transmission and lack of mechanical strength of the carrier collagen. Implants incorporating BMP are also expensive owing to the need for high doses of BMP-2 and would be a barrier to widespread use of such

implants. Safe and cost-effective local delivery systems for BMPs avoiding these problems would be important. Better delivery systems and/or ways to reduce the required BMP dose by enhancing BMP action [24, 27, 33, 38] are possible solutions. At the same time, it is important to reduce the cost of production of recombinant human BMP-2 for widespread clinical use of rhBMP-2. The efficiency of production of BMP-2 with E. coli [18, 29] appears superior to that with animal cells, and might provide less expensive BMP-2 for practice use.

We therefore asked whether E. coli-derived rhBMP-2 (E-BMP-2)-adsorbed porous β-TCP granules could achieve posterolateral lumbar fusion in a rabbit model similar to autogenous bone graft as judged by radiographic fusion, mechanical stiffness and histologically evident fusion mass.

Materials and Methods

We used 68 New Zealand white rabbits 18 weeks of age (weight, 2.8–3.2 kg) in this experimental study. Of these, 52 rabbits were equally divided into four groups (13 per group) by dose of E-BMP-2 adsorbed to β-TCP granules (Table 1). Eight rabbits were used as negative controls (implantation of β-TCP granules alone without E-BMP-2) and the remaining eight had only autogenous bone grafting. Posterolateral lumbar spinal fusion was performed with autogenous bone or β-TCP granules adsorbed with five different doses of E-BMP-2. Efficacy of E-BMP-2 for lumbar spinal fusion was evaluated with CT for new bone formation and with fusion scores, the bending load of the fusion required to create 1-mm middle-span deflection, and histological examination with von Kossa staining for mineralization, toluidine blue and TRAP staining for cartilage formation and β-TCP resorption. This protocol including animal care was approved by the Institutional Committee for Animal Care and Experiments of Osaka City University Medical School.

Table 1. Implant assignment

Group	Total number	Number harvested		E-BMP-2 (μg/side)	β-TCP (μg/side)
		At 4 weeks	At 8 weeks		
Autogenous bone graft	8	0	8	–	–
BMP0	8	0	8	0	500
BMP5	13	5	8	5	500
BMP15	13	5	8	15	500
BMP50	13	5	8	50	500
BMP150	13	5	8	150	500

E-BMP-2 with dimeric molecular structure was produced in human BMP-2 gene-transfected E. coli with monomeric structure and stored in inclusion bodies, which were collected. The molecular structure was unfolded in protein-denaturing agents, and then refolded to form dimeric E-BMP-2 by removal of denaturing agents. Dimeric E-BMP-2 was purified by several steps of chromatography. Details of the procedures for dimerization of cytokines have already been reported [29, 40].

We anesthetized the animals with an intramuscular injection of ketamine (30 mg/kg) and xylazine (10 mg/kg). Flomoxef sodium (60 mg) was administered intramuscularly as a prophylactic antibiotic. Each rabbit underwent a single-level posterolateral intertransverse process fusion at L5–L6. We made a dorsal midline skin incision followed by two paramedian fascial incisions on both sides. The intermuscular plane between the multifidus and longissimus muscles was retracted to expose both transverse processes of L5–L6 and the intertransverse membranes. We used an electric-driven burr (Stryker, Kalamazoo, MI) to decorticate the posterior cortex of the transverse processes, and one of the implant or transplant materials was implanted in both sides (one implant per side). The wounds were then closed with 3–0 nylon sutures and skin staples. After surgery, rabbits had free access to food and water the same as before surgery.

To create the implants, E-BMP-2 freeze-dried powder was dissolved in distilled water to reconstitute before use. We used interconnecting porous β-TCP granules 1 mm to 3 mm in diameter (pore size, 50–350 μm; porosity, 75%) (HOYA Corp, Tokyo, Japan). To prepare one implant to bridge the sides between transverse processes of L5 and L6, 500 mg of β-TCP granules were soaked in 500 μl of distilled water containing one of various dosages of E-BMP-2 (5, 15, 50, or 150 μg) for more than 15 minutes at room temperature. Implants with 500 mg of β-TCP granules soaked with 500 μl of distilled water without E-BMP-2 served for controls. Adsorbance of β-TCP was established by determining the concentration of protein in supernatant after centrifugal separation using Bio-Rad protein assay dye reagent concentrate (Bio-Rad Laboratories, Inc., Hercules, CA). Based on the results of preliminary experiments, it was estimated less than 10% of E-BMP-2 was collected from the supernatant. Autogenous bone chips harvested from the iliac crest (0.8–1 g/side) were also prepared as positive controls.

Four weeks after surgery, five animals from each group were sacrificed by overdose of pentobarbital sodium (50 mg/kg), and the L4–L7 lumbar spines were harvested and processed for further examination. At 8 weeks after surgery, the remaining animals from the experimental and control groups (eight animals per group) were sacrificed and processed in the same fashion.

The lumbar spines were examined for fusion mass condition by anteroposterior plain radiography and CT (GE Yokogawa Medical System, Tokyo, Japan) at 1-mm slice thickness to construct 3-D images every 2 weeks and harvested with dissection of soft tissue at each time point. Fusion was evaluated on sagittal CT view 10 mm lateral from the midline. Three independent observers (SD, TM and HY), who were all spine surgeons, judged the fusions using the following standardized scale: 0 = no bone formation and of β-TCP or transplanted bone absorption between transverse processes, 1 = some bone formation between transverse processes, but β-TCP or transplanted bone absorption was incomplete, 2 = continuous bone bridging between transverse processes and β-TCP or transplanted bone absorption was complete. All three observers agreed on all observations.

Mechanical testing to evaluate the solidity of the L5–L6 fusion site was performed by a three-point flexion-bending test using a materials testing machine (Instron 5882, Instron, Boston, MA). The superior and inferior ends of samples were flattened by trimming, and samples were horizontally held in the apparatus. Three-point bending tests were performed with a 30-mm intersupport distance and a 1 mm/minute head speed. The bending load at 1-mm middle-span deflection was determined from the load-deflection curves.

The specimens harvested at 8 weeks (n = 3 from each group) after surgery were fixed in 4% paraformaldehyde overnight at 4°C, dehydrated in a graded ethanol series, and embedded in plastic resin. Sections 7 μm in thickness in the region of the intertransverse process were cut in the sagittal plane with a tungsten blade using a rotary microtome (RM2255, Leica Microsystems, Wetzlar, Germany) and stained with hematoxylin and eosin (H-E) after decalcification with 0.5 M EDTA for 30 minutes at room temperature, and stained with toluidine blue and von Kossa and van Gieson staining without decalcification. We examined four sections from each sample taken 10 mm lateral from the midline. Amounts of β-TCP in new bone were observed microscopically; area of residual β-TCP were identified manually using software specialized for bone histomorphometry, OsteoMeasure (Osteometrics Inc, Decatur, GA), and expressed per square micron (μm^2). To identify osteoclasts that might have resorbed β-TCP within newly formed bone masses, tartrate-resistant acid phosphatase (TRAP) staining was performed on three sections from specimens taken from each of the five groups of animals sacrificed at 4 weeks after implantation.

We determined differences in the radiographic score, bending load, and histomorphometric measures between the autogenous bone graft group and each of the four E-BMP-2 treatment groups using the Kruskal-Wallis test and the post-hoc Scheffe test. We used StatView-J 5.0 (SAS Institute Inc, CA, USA) for all analyses.

Results

E-BMP-2-adsorbed porous β-TCP granules achieved posterolateral lumbar fusion same as autogenous bone graft evaluated by 3-D CT images (Fig. 1A) and plain radiographs (data not shown). The β-TCP granules appeared replaced by calcified mass with flat surface in E-BMP-2 dose- and time-dependent fashion, though β-TCP granules of the control group without E-BMP-2 continued to be observed throughout the observation period. Moreover, the radiographic scores showed treatment with 15 μg/side of E-BMP-2 achieved spinal fusion similar to autogenous bone graft, and that higher scores were obtained with 50 and 150 μg/side of E-BMP-2 than for the autogenous bone graft control (Fig. 1B).

The bending load required to produce 1-mm middle-span deflection of the fusion mass for the BMP15 group was similar to that of the autogenous bone graft control group (Fig. 2). The bending load of the specimens from the BMP50 and BMP150 groups were higher than those in the autogenous bone graft control group (Fig. 2). Specimens from animals with the β-TCP granules retaining E-BMP-2 (50 μg/side or more) had in a larger bending load than that from animals treated with autogenous bone grafts.

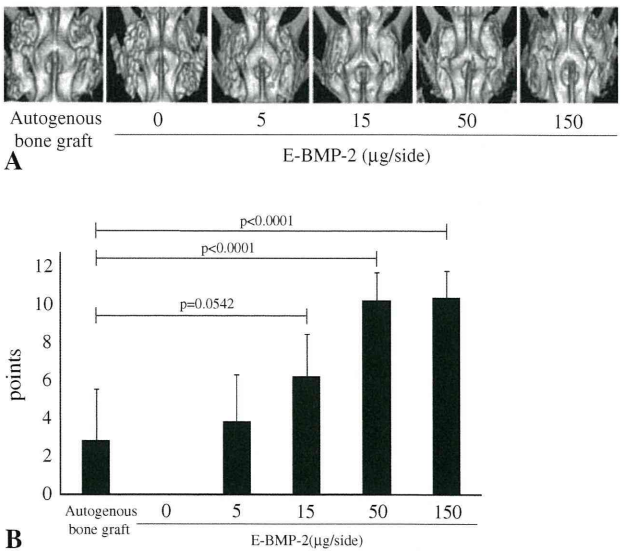

Fig. 1A–B (**A**) Representative 3D-CT images of posterolateral fusion at 8 weeks after surgery are shown. Fusion masses of groups of BMP15, BMP50 and BMP150 are well remodeled as is the autogenous bone graft group. E-BMP-2 treatment could radiographically achieve lumbar spinal fusion the same as autogenous bone graft. (**B**) Radiological fusion scores of 3D-CT of BMP50 and BMP150 were higher than autogenous bone graft control group. Values are mean ± standard deviation (SD).

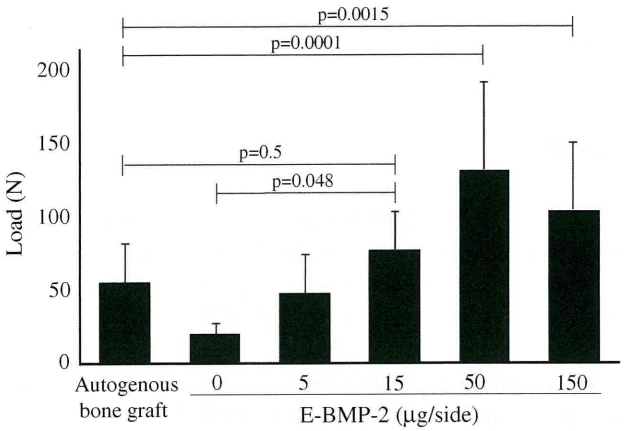

Fig. 2 The bending load at 1-mm middle-span deflection of the fusion mass of the BMP15 group was similar to that of autogenous bone graft control group. More than 15 μg/side of E-BMP-2 treatment could mechanically achieve lumbar spinal fusion as well as autogenous bone graft. The bending loads of the BMP50 and BMP150 were higher than that of the autogenous bone graft control group. Values are mean ± SD.

Histological examination revealed E-BMP-2 adsorbed β-TCP granules achieved fusion between transverse processes as well as autogenous bone graft. Eight weeks after operation, the bone masses with the peripheral cortical bone bridging the transverse processes achieved with more than 50 μg/side of E-BMP-2 (Fig. 3D, E, J and G) were similar to those achieved with autogenous bone graft (Fig. 3F and L) although the groups treated with less than 15 μg/side of E-BMP-2 (Fig. 3A–C, G–I) could not be achieved complete bone bridging. Toluidine blue-stained specimens from the groups of BMP5, BMP15, and the autogenous bone grafting control group (Fig. 4B and H, C and I, F and L, respectively) revealed metachromatic cartilage formation in the middle of the new bony mass bridging the transverse processes though there is no cartilage residue in the bone mass between transverse processes of the groups treated with more than 50 μg/side of E-BMP-2 (Fig. 4D and E). Higher-magnification views of bridging bone masses showed remaining β-TCP granules in these groups (Fig. 4G–K). In the controls without E-BMP-2, only fibrous tissue and remaining β-TCP without new bone were seen (Fig. 4A and G). The amount of β-TCP remaining within new bone mass was reduced ($p < 0.0001$) in all BMP groups compared with the control group treated without E-BMP-2 (Fig. 5). Furthermore, within newly formed bone in the E-BMP-2-treated groups (Fig. 6A–D), osteoclasts (TRAP-positive giant cells) were predominantly seen on the surfaces of the β-TCP in a dose dependent manner (Fig. 6E–H), suggesting more rapid resorption of β-TCP within the BMP-induced new bone mass and remodeling of the fusion masses.

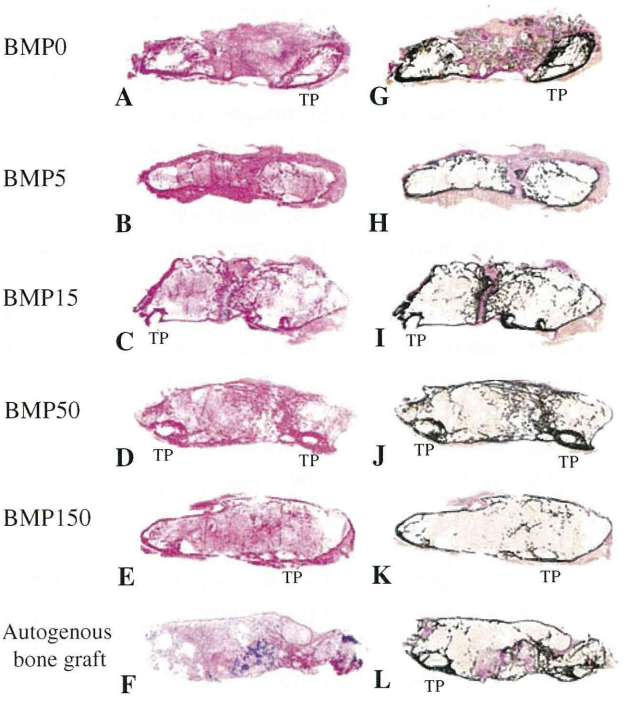

Fig. 3A–L Representative longitudinal histology sections of fusion mass of each group 8 weeks after surgery are shown. (**A**) BMP0; (**B**) BMP5; (**C**) BMP15; (**D**) BMP50; (**E**) BMP150; (**F**) autogenous bone graft (Stain, hematoxylin and eosin; original magnification, ×1). (**G**) BMP0; (**H**) BMP5; (**I**) BMP15; (**J**) BMP50; (**K**) BMP150; (**L**) autogenous bone graft (Stain, von Kossa and van Gieson; original magnification, ×1). Newly formed bone mass between transverse processes of BMP50 and 150 showed completely continuous cortical bone as well as autogenous bone graft control group. More than 50 μg/side of E-BMP-2 treatment could histologically achieve lumbar spinal fusion as well as autogenous bone graft.

Discussion

BMPs were originally identified as osteoinductive proteins by Urist more than 40 years ago. Since cloning of BMP genes, studies of BMPs and their clinical application have advanced. However, with progression of clinical application, issues related to drug delivery systems and production costs have arisen. β-TCP granules are widely used in clinical situations and E. coli-derived rhBMP-2 (E-BMP-2) can be produced at less cost compared with mammalian cell-derived BMP-2. Therefore we asked whether E. coli-derived rhBMP-2 (E-BMP-2) adsorbed on porous β-TCP granules could achieve posterolateral lumbar fusion in a rabbit model similar to that of autogenous bone graft.

We note several limitations. First, we used a rabbit posterolateral spinal fusion model. For clinical application, studies must be performed in much larger animals including sheep or nonhuman primates since the efficacy of cytokines and BMPs vary in differing species. Second, we followed the process of spinal fusion for only 8 weeks. Although this time period was determined by longitudinal